Molecular transistor coupled to phonons and Luttinger-liquid leads

So Takei[1], Yong Baek Kim[1,2], and Aditi Mitra[3]
[1]*Department of Physics, University of Toronto, Toronto, Ontario M5S 1A7, Canada*
[2]*School of Physics, Korea Institute for Advanced Study, Seoul 130-722, Korea*
[3]*Department of Physics, Columbia University, New York, New York 10027*
(Dated: August 2, 2021)

We study the effects of electron-phonon interactions on the transport properties of a molecular quantum dot coupled to two Luttinger-liquid leads. In particular, we investigate the effects on the steady state current and DC noise characteristics. We consider both equilibrated and unequilibrated on-dot phonons. The density matrix formalism is applied in the high temperature approximation and the resulting semi-classical rate equation is numerically solved for various strengths of electron-electron interactions in the leads and electron-phonon coupling. The current and the noise are in general smeared out and suppressed due to intralead electron interaction. On the other hand, the Fano factor, which measures the noise normalized by the current, is more enhanced as the intralead interaction becomes stronger. As the electron-phonon coupling becomes greater than order one, the Fano factor exhibits super-Poissonian behaviour.

PACS numbers: 73.63.Kv, 71.10.Pm, 74.20.Mn

I. INTRODUCTION

In the relentless search for smaller electronic devices, the idea of fabricating extremely small transistors using quantum dots has become an important topic. In recent years, the possibility of using a very small molecule as the quantum dot in a transistor has become apparent[1,2,3,4,5,6,7,8,9]. Such a device may be thought of as a molecular quantum dot weakly coupled to macroscopic charge reservoirs, or leads.

Molecules integrated into these transistors often have very complex structures and therefore introduce new electronic transport properties. For example, the shape of the molecule or the position of the molecule relative to the leads can change as charges are added onto the molecule. A number of experiments have investigated the effects of coupling between tunneling electrons and the on-dot vibrational quanta on various transport properties of the molecule[9,10,11,12]. Of particular interest is the experimental evidence for electron-phonon coupling in a molecular device composed of C_{60} molecule deposited between a pair of gold electrodes[12]. Experimental results show peaks in the differential conductance which may be due to the effect of coupling between tunneling electrons and the molecular vibrational mode.

Several theoretical works[13,14,15,16,17,18,19,20] have harnessed the study of electron-phonon coupling by introducing an on-dot phonon degree of freedom that couples to on-dot electrons and observed the effects the coupling has on various transport properties of the molecular transistor. One of the most recent comprehensive work on phonon effects in molecular transistors coupled to two *non-interacting* leads was conducted by Mitra *et al.*[13]. They developed the density matrix formalism to study transport properties for both in-equilibrium and out-of-equilibrium phonon distributions.

In our work, we investigate how the phonon distribution *and* electron-electron interaction in the leads affect the steady state DC current and the DC noise characteristics of a molecular transistor. The phonon distribution can drastically change depending on how they are allowed to relax as they couple onto a bath. As discussed in Mitra *et al.*[13], we must consider two competing time scales: time scale for the phonons to reach equilibrium via their interaction with the bath, $\tau_{\rm ph}$; and the dwell time of the electron on the dot, $\tau_{\rm dwell}$. The two limiting cases considered in this work are: the phonons are equilibrated to the bath corresponding to $\tau_{\rm dwell} \gg \tau_{\rm ph}$; and the opposite case where the tunneling electrons see unequilibrated phonons corresponding to $\tau_{\rm ph} \gg \tau_{\rm dwell}$.

We are particularly interested in the effects of electron-electron interaction in the leads. Up to this date, theoretical works have only considered non-interacting electrons in the leads. This is sufficient if the leads are two or three dimensional electron gases, where interactions affect the low energy properties of the lead only perturbatively. However, in one dimension, arbitrarily weak electron interaction completely changes the ground state. In our work, we consider the leads to be a Luttinger liquid. Our work may represent a physical device composed of a molecular quantum dot, such as C_{60}, coupled to two metallic single-walled carbon nanotubes, which behave essentially as interacting one-dimensional objects.

The outline of this paper is as follows. We consider a molecule with a single level coupled to two Luttinger-liquid leads. We suppose that the electrons are coupled to the on-dot vibrational mode and consider both equilibrated and unequilibrated phonons. We solve the model in the density matrix formalism and apply the high-temperature approximation. The approximation will be used to derive the rate equation for the dot occupation probabilities and use the equation to compute the steady state DC current and the DC noise characteristics of the molecular transistor as a function of source-drain voltage. In section II, we introduce our model, provide a brief outline of the density matrix formalism, and present expressions for the tunneling current and the DC noise. In section III, we present numerical results for the cur-

rent and the noise and discuss the dependence of these transport properties on the phonon distribution and the intralead electron interaction. We conclude in section IV.

II. FORMULATION OF THE PROBLEM

A. Model

Our model considers a molecule with a single non-degenerate energy level, of energy ϵ_0, coupled to two Luttinger-liquid leads labelled L (left) and R (right). We allow the tunneling electrons to couple to a single phonon mode, with frequency ω_0 corresponding to the internal vibrational mode of the molecule. The full Hamiltonian is given by

$$H = H_{dot} + H_{leads} + H_t, \tag{1}$$

where H_{dot} describes the on-dot electrons coupled to the single phonon mode, H_{leads} represents the electrons in the leads, and H_t corresponds to the tunneling between the dot and the leads.

More specifically, H_{dot} has the form,

$$H_{dot} = \epsilon_0 \sum_\sigma c_\sigma^\dagger c_\sigma + \frac{U}{2} \sum_\sigma c_\sigma^\dagger c_\sigma \left(\sum_\sigma c_\sigma^\dagger c_\sigma - 1 \right) + \lambda\omega_0 \left(b^\dagger + b\right) \sum_\sigma c_\sigma^\dagger c_\sigma + \omega_0 b^\dagger b, \tag{2}$$

where $c_\sigma^\dagger$ is the creation operator of electrons with spin σ on the dot and $b^\dagger$ is the creation operator of the on-dot phonons. λ is the electron-phonon coupling strength and U is the charging energy of the molecule. Our work focuses on the limit $U \to \infty$, which may be relevant when considering the case of C_{60} transistors whose charge states are most likely zero or one[12,26]. H_{leads} and H_t are given by

$$H_{leads} = \sum_{i=L,R} H_{lead-i} = \sum_i H_{kin-i} + H_{int-i}, \tag{3}$$

and

$$H_t = \sum_{\substack{k,\sigma \\ i=L,R}} \left[t_i (a_{i,k,\sigma}^\dagger + b_{i,k,\sigma}^\dagger) c_\sigma + h.c. \right], \tag{4}$$

where

$$H_{kin-i} = v_F \sum_{k,\sigma} \Big[(k - k_F) a_{k,\sigma,i}^\dagger a_{k,\sigma,i} - (k + k_F) b_{k,\sigma,i}^\dagger b_{k,\sigma,i} \Big] \tag{5}$$

$$H_{int-i} = \frac{1}{2L_s} \sum_{q,k,k',\sigma,\sigma'} \Big\{ 2g_2 a_{k+q,\sigma,i}^\dagger a_{k,\sigma,i} b_{k'-q,\sigma',i}^\dagger b_{k',\sigma',i} + g_4 \Big[a_{k+q,\sigma,i}^\dagger a_{k,\sigma,i} a_{k'-q,\sigma',i}^\dagger a_{k',\sigma',i} + b_{k-q,\sigma,i}^\dagger b_{k,\sigma,i} b_{k'+q,\sigma',i}^\dagger b_{k',\sigma',i} \Big] \Big\}. \tag{6}$$

H_{kin-i} and H_{int-i} respectively correspond to the kinetic and the interaction terms of the electrons in lead i; L_s is the linear size of the leads, and v_F (k_F) is the Fermi velocity (wavevector). Here $a_{k,\sigma,i}^\dagger (b_{k,\sigma,i}^\dagger)$ creates a right(left)-moving electron with momentum k and spin σ on lead i. g_2 and g_4 represent forward scatterings; in our work, we will not consider the back-scattering interaction.

In the absence of back-scattering, the Luttinger Hamiltonian, H_{lead-i}, is exactly soluble using the technique of bosonization[23,24,25]. First, we rewrite the Hamiltonian using the Fourier components of the particle density operator for right and left movers:

$$\rho_{+,\sigma,i}(q) = \sum_k a_{k+q,\sigma,i}^\dagger a_{k,\sigma,i}, \tag{7}$$

$$\rho_{-,\sigma,i}(q) = \sum_k b_{k+q,\sigma,i}^\dagger b_{k,\sigma,i}. \tag{8}$$

In the continuum limit ($L_s \to \infty$),

$$H_{kin-i} = v_F \int_0^\infty \sum_\sigma dq \left[\rho_{+,\sigma,i}(q)\rho_{+,\sigma,i}(-q) + \rho_{-,\sigma,i}(-q)\rho_{-,\sigma,i}(q) \right], \tag{9}$$

$$H_{int-i} = \frac{1}{2\pi} \int dq \sum_{\sigma,\sigma'} \Big\{ g_2 \rho_{+,\sigma,i}(q)\rho_{-,\sigma',i}(-q) + \frac{g_4}{2} \left[\rho_{+,\sigma,i}(q)\rho_{+,\sigma',i}(-q) + \rho_{-,\sigma,i}(-q)\rho_{-,\sigma',i}(q) \right] \Big\}. \tag{10}$$

In order to express the Hamiltonian in diagonal form, we introduce the canonically conjugate Boson operators, $\phi_{\sigma,i}$ and $\Pi_{\sigma,i}$,

$$\phi_{\sigma,i}(x) = -\frac{i}{2} \int_{q\neq 0} \frac{dq}{q} e^{-\frac{\alpha|q|}{2} - iqx} \left[\rho_{+,\sigma,i}(q) + \rho_{-,\sigma,i}(q) \right] \tag{11}$$

and

$$\Pi_{\sigma,i}(x) = \frac{1}{2\pi} \int_{q\neq 0} dq e^{-\frac{\alpha|q|}{2} - iqx} \left[\rho_{+,\sigma,i}(q) - \rho_{-,\sigma,i}(q) \right], \tag{12}$$

where α is a small convergence factor or the inverse of a large ultraviolet cutoff. These operators are transformed into the charge and spin boson operators,

$$\phi_{c(s),i} = \frac{\phi_{\uparrow,i} + (-)\phi_{\downarrow,i}}{\sqrt{2}}, \tag{13}$$

$$\Pi_{c(s),i} = \frac{\Pi_{\uparrow,i} + (-)\Pi_{\downarrow,i}}{\sqrt{2}}, \tag{14}$$

which obey

$$[\phi_{\mu,i}(x), \Pi_{\nu,i}(y)] = i\delta_{\mu,\nu}\delta(x-y). \tag{15}$$

The single fermion operators for right- and left-moving electrons with spin σ on lead i can be written in position representation as

$$\psi_{\pm,\sigma,i}(x) = \lim_{\alpha\to 0}\frac{1}{\sqrt{2\pi\alpha}}e^{\pm ik_F x - i\frac{1}{\sqrt{2}}[\pm(\phi_{c,i}+\sigma\phi_{s,i})+(\theta_{c,i}+\sigma\theta_{s,i})]}, \quad (16)$$

where

$$\theta_{\mu,i} = \pi\int^x dx'\Pi_{\mu,i}(x'). \quad (17)$$

The Hamiltonian, H_{lead-i}, can be expressed in terms of the canonically conjugate charge and spin boson operators (Eqs.13,14) as,

$$H_{lead-i} = \sum_{\mu=c,s}\frac{v_\mu}{2}\int dx\left[\pi K_\mu\Pi_{\mu,i}^2 + \frac{1}{\pi K_\mu}(\partial_x\phi_{\mu,i})^2\right], \quad (18)$$

where

$$v_c = \sqrt{\left(v_F+\frac{g_4}{\pi}\right)^2 - \left(\frac{g_2}{\pi}\right)^2}; \quad (19)$$

$$K_c = \sqrt{\frac{\pi v_F + g_4 - g_2}{\pi v_F + g_4 + g_2}}; \quad (20)$$

$$v_s = v_F; \quad (21)$$

$$K_s = 1. \quad (22)$$

Notice that $K_c < 1$ ($K_c > 1$) for repulsive (attractive) interaction.

Now a convenient canonical transformation[22] can be applied on the full Hamiltonian making it diagonal in the dot variables. The desired transformation is $H \to H' = e^s H e^{-s}$ where

$$s \equiv \lambda\sum_\sigma c_\sigma^\dagger c_\sigma\left(b^\dagger - b\right) = -s^\dagger. \quad (23)$$

Then, the transformed Hamiltonian is given by

$$H' = H'_{dot} + H_{leads} + H'_t, \quad (24)$$

where

$$H'_{dot} = \epsilon'\sum_\sigma c_\sigma^\dagger c_\sigma + \frac{U'}{2}\sum_\sigma c_\sigma^\dagger c_\sigma\left(\sum_\sigma c_\sigma^\dagger c_\sigma - 1\right) + \omega_0 b'^\dagger b', \quad (25)$$

and

$$H'_t = \sum_{\substack{k,\sigma\\ i=L,R}}\left[t_i e^{-\lambda(b^\dagger - b)}(a_{i,k,\sigma}^\dagger + b_{i,k,\sigma}^\dagger)c_\sigma + h.c.\right]. \quad (26)$$

The transformed phonon operator is

$$b' = b - \lambda\sum_\sigma c_\sigma^\dagger c_\sigma, \quad (27)$$

which shows that ground state energy of the phonon spectrum depends on electron occupancy of the dot. The shifted energy level of the molecule is $\epsilon' = \epsilon_0 - \lambda^2\omega_0$, while the shifted charging energy, U', is not explicitly shown since we only consider the limit $U \to \infty$.

B. Formalism

1. The high-temperature approximation

The spirit of the high-temperature approximation stems from the presence of two competing energy scales: the temperature, k_BT, and the tunneling rate of an electron from a lead onto the dot (or vice versa), $h\Gamma$. In the approximation, one assumes that $k_BT \gg h\Gamma$. Low tunneling rate infers that the number of charges on the dot is a well-defined integer, and thus one can characterize the state of the dot by a set of dot occupational probabilities. The equation of motion of these dot occupational probabilities is the rate equation. In fact, a dot-lead system can be tuned into the low tunneling regime in certain experiments[12].

2. The rate equation

The central element in determining the transport properties of our molecular transistor in the high-temperature approximation is the semi-classical rate equation, which are the equations of motion for the various occupational probabilities of the dot. To obtain the rate equation, we use the density matrix formalism, developed by Mitra *et al.*[13], which allows us to determine probabilities for various states of the dot under both equilibrium and out-of-equilibrium conditions.

We start with the full density matrix ρ that obeys the equation of motion

$$\dot\rho = -i[H,\rho]. \quad (28)$$

The initial step is to assume that the leads are in equilibrium independent of the molecular state. To harness this assumption, we express ρ as the sum of the projected density matrix,

$$\rho_s = \mathrm{Tr}_{leads}\{\rho(t)\}\otimes\rho_{leads}, \quad (29)$$

and the complementary density matrix

$$\rho_t = \rho - \rho_s. \quad (30)$$

Here, ρ_{leads} is the density matrix of the two leads at thermal equilibrium with chemical potential μ_L for the left lead and μ_R for the right lead. Tr_{leads} denotes tracing over the leads degree of freedom. On physical grounds, this decomposition is useful because the diagonal components of the reduced density matrix, $\rho_D \equiv \mathrm{Tr}_{leads}\{\rho_s\}$, relate directly to the occupational probabilities of various states of the dot. In the high-temperature approximation, the equation of motion for ρ_s, using Eqs.28,29, can be written as

$$\dot\rho_{sI}(t) \approx -i\mathrm{Tr}_{leads}[H_{tI}(t),\rho_{tI}(t)]\otimes\rho_{leads}, \quad (31)$$

where subscript I indicates that the operators are in the interaction picture: $O_I(t) = e^{iH_0t}O(t)e^{-iH_0t}$, where

$H_0 \equiv H_D + H_{leads}$. Eq.31 indicates that the time evolution of ρ_s is coupled to ρ_t and vice versa. However, one can show that the equations of motion for ρ_s and ρ_t can be decoupled in the high temperature approximation[13], leading to

$$\frac{d\rho_s(t)}{dt} = \frac{d(\rho_D \otimes \rho_{leads})}{dt} \approx -\frac{1}{2}\int_{-\infty}^{\infty} d\tau \left[H_t, e^{-iH_0(t-\tau)}[H_t, \rho_s(t)]e^{iH_0(t-\tau)}\right]. \quad (32)$$

By tracing out the leads degree of freedom on both sides of Eq.32, one obtains coupled equations of motion for the various occupational probabilities of the dot. Identifying P_q^n as the probability for the dot to be in a state with n electrons and q phonons,

$$P_q^n = \langle n, q|\rho_D|n, q\rangle, \quad (33)$$

we arrive at the rate equation,

$$\begin{aligned}\dot{P}_q^n = \sum_{\substack{i=L,R\\p}} & 2n_i\left((q-p)\omega_0 + U(n-1)\right)\Gamma_{q,p}^i P_p^{n-1} \\ & + \bar{n}_i\left((p-q)\omega_0 + Un\right)\Gamma_{q,p}^i P_p^{n+1} \\ & - \bar{n}_i\left((q-p)\omega_0 + U(n-1)\right)\Gamma_{p,q}^i P_q^n \\ & - 2n_i\left((p-q)\omega_0 + Un\right)\Gamma_{p,q}^i P_q^n,\end{aligned} \quad (34)$$

where

$$\Gamma_{q<p}^i = t_i^2 N_0 \left|\sum_{l=0}^{q} \frac{(\lambda^2)^l\sqrt{q!p!}\lambda^{|q-p|}e^{-\lambda^2/2}}{l!(q-l)!(l+|p-q|)!}\right|^2, \quad (35)$$

$$\begin{aligned} n_i(\omega) &= \frac{1}{N_0}\int_{-\infty}^{\infty} dt e^{i\omega t}\langle\psi_{i,\sigma}^\dagger(0)\psi_{i,\sigma}(t)\rangle \\ &= \frac{e^{\frac{-(\epsilon'+\omega-\mu_i)}{2T}}}{2\pi}\left(\frac{2\pi T\alpha}{v_c}\right)^{\beta-1}\times \\ &\quad \times \frac{\left|\Gamma\left(\frac{\beta}{2}+\frac{i(\epsilon'+\omega-\mu_i)}{2\pi T}\right)\right|^2}{\Gamma(\beta)}, \end{aligned} \quad (36)$$

$$\begin{aligned} \bar{n}_i(\omega) &= \frac{1}{N_0}\int_{-\infty}^{\infty} dt e^{i\omega t}\langle\psi_{i,\sigma}(t)\psi_{i,\sigma}^\dagger(0)\rangle \\ &= \frac{e^{\frac{\epsilon'+\omega-\mu_i}{2T}}}{2\pi}\left(\frac{2\pi T\alpha}{v_c}\right)^{\beta-1}\times \\ &\quad \times \frac{\left|\Gamma\left(\frac{\beta}{2}+\frac{i(\epsilon'+\omega-\mu_i)}{2\pi T}\right)\right|^2}{\Gamma(\beta)}, \end{aligned} \quad (37)$$

where $N_0 = (v_c v_F)^{-1/2}$. $\Gamma_{q,p}^i$ denotes the rate at which an electron on the dot hops off onto lead i or an electron on lead i hops onto the dot while the dot phonon occupancy changes from q to p during the process; it is symmetric under the interchange of q and p. $\Gamma(z)$ is the gamma function, while $n(\omega)$ is the electron occupation number for interacting electrons and is analogous to the Fermi distribution, $f(\omega)$ for non-interacting electrons ($\bar{n}(\omega)$ is analogous to $(1-f(\omega))$). The factors of 2 in the first and the last terms in Eq.34 are due to electron's spin degree of freedom. The exponent β is given by

$$\beta = \frac{1}{4}\left(K_c + \frac{1}{K_c}\right) + \frac{1}{2}. \quad (38)$$

In the non-interacting limit, $K_c = 1$ and hence $\beta = 1$. However, for *any* non-vanishing interaction, $K_c \neq 1$ and hence $\beta > 1$.

The general form of the rate equation is the same as the original rate equation for the case of non-interacting leads[13]. However, notice that when the interaction in the leads is taken into account, the Fermi functions, $f(\omega)$, in the original rate equation, is replaced by the Luttinger-liquid distribution function, $n(\omega)$.

In the limit $U \to \infty$, n in Eq.34 is either 0 or 1. During numerical calculations, we allow q to take on values between 0 and some large cut-off, $q_{max} \gg 1$. In this case, P_q^n is a vector of length $2q_{max}$, and the rate equation can be expressed in matrix form,

$$\dot{\mathbf{P}} = \mathcal{M}\mathbf{P}, \quad (39)$$

where $\mathcal{M}$ is a $2q_{max}\times 2q_{max}$ matrix. At steady state, $\dot{\mathbf{P}} = 0$, so the solution for $\mathbf{P}$ is the eigenvector corresponding to the zero eigenvalue of $\mathcal{M}$. For equilibrated phonons, we use the ansatz[13],

$$P_q^n = P^n e^{-q\omega_0/T}(1 - e^{-\omega_0/T}). \quad (40)$$

where P^0 is the probability that the dot is empty and $P^1 = 1 - P^0$.

3. I-V characteristics

In the density matrix formalism, current through lead i is given by

$$\langle I_i\rangle = \mathrm{Tr}\{\rho(t)\hat{I}_i\} = \mathrm{Tr}\{\rho_t(t)\hat{I}_i\}, \quad (41)$$

where the current operator is

$$\hat{I}_i = it_i\sum_{k,\sigma}\left[e^{-\lambda(b^\dagger - b)}(a_{i,k,\sigma}^\dagger + b_{i,k,\sigma}^\dagger)c_\sigma - h.c.\right]. \quad (42)$$

Performing the trace over the leads and the dot degrees of freedom, we can express the steady state current in terms of dot occupational probabilities, P_q^n. In the limit $U \to \infty$, we get

$$\begin{aligned}\langle I_i\rangle = \sum_{q,p}\big[&2P_q^0 n_i((p-q)\omega_0)\Gamma_{q,p}^i \\ &- P_q^1\bar{n}_i((q-p)\omega_0)\Gamma_{p,q}^i\big].\end{aligned} \quad (43)$$

4. DC noise characteristics

It is also interesting to see how the second moment in current is affected by the electron-phonon coupling and electron-electron interactions in the leads. Current through the molecular transistor fluctuates even when the system is subject to a DC bias. These current fluctuations, or noise, can be characterized by the zero frequency component of the Fourier transform $\tilde{S}(\omega)$ of the current correlation function,

$$\begin{aligned} S_{LL}(t) &= \frac{1}{2}\langle[\delta I_L(t), \delta I_L(0)]_+\rangle \\ &= \frac{1}{2}\mathrm{Tr}\{\rho(I_L(t)I_L(0) + I_L(0)I_L(t))\} \\ &\quad - \left[\mathrm{Tr}\{\rho I_L\}\right]^2, \end{aligned} \tag{44}$$

where $\delta I_i(t) = I_i(t) - \langle I_i(t)\rangle$. Charge conservation implies $I_L = -I_R$. Therefore, the current fluctuations are equal at both leads, giving $S_{LL}(t) = S_{RR}(t)$. Therefore, it suffices to compute the current correlation only at the left lead.

In the Heisenberg picture, current evolves over time as per $I_L(t) = e^{iHt} I_L(0) e^{-iHt}$. Substituting this into Eq.44, we get

$$S_{LL}(t) = \frac{1}{2}\mathrm{Tr}\{R(t) I_L(0)\}, \tag{45}$$

where

$$R(t) = e^{-iHt}\left[\delta I_L(0)\rho + \rho\delta I_L(0)\right] e^{iHt}. \tag{46}$$

Since $S_{LL}(t) = S_{LL}(-t)$, $S_{LL}(t)$ will be computed only for positive time. The equation of motion for the causal function $R(t)$ can be obtained from the equation of motion for the density matrix and is given by

$$\begin{aligned} &\dot{R}(t) = \\ &\quad -i[H, R(t)] + \delta(t)[\delta I_L(0)\rho + \rho\delta I_L(0)], \quad t \geq 0, \end{aligned} \tag{47}$$

and is zero elsewhere. Solving the equation of motion for $R(t)$ is similar to the procedure for solving the density matrix equation of motion (section II B 2). First, we decompose the causal function into the diagonal component in the dot and leads variables, and the off-diagonal component in those variables: $R = R_s + R_t$, where $R_s = R_D \otimes R_{leads}$ with $R_D \equiv \mathrm{Tr}_{leads}\{R_s\}$. From Eq.47, we obtain the equation of motion for $R_s(t)$ in the high-temperature approximation,

$$\dot{R}_s(t) \approx -i[H_t, R_t] + \delta(t)\left(I\rho_t + \rho_t I - 2\langle I\rangle\rho_s\right). \tag{48}$$

Notice that the time evolution of R_s couples to R_t. The coupled equations of motion for R_s and R_t can be decoupled in the high temperature approximation. Then, as was done for the density matrix, we trace out the leads degree of freedom in the decoupled equation of motion for R_s and arrive at the equation of motion for R_D.

$$\dot{\mathbf{R}}_D(t) = \mathcal{M}\mathbf{R}_D + \delta(t)\mathbf{h}, \tag{49}$$

where $\mathcal{M}$ is the same matrix as the one appearing in Eq.39 and vector $\mathbf{h}$ is given by

$$\begin{aligned} h_q^n &= -2\langle I_L\rangle P_q^n \\ &\quad + 2\sum_p \left[(3-n)P_p^{n-1} n_L((q-p)\omega_0 + U(n-1))\Gamma_{q,p}^L\right. \\ &\qquad \left. -(n+1)P_p^{n+1}\bar{n}_L((p-q)\omega_0 + Un)\Gamma_{q,p}^L\right]. \end{aligned} \tag{50}$$

The final step is to express the DC noise in terms of dot occupational probabilities and the components of $\mathbf{R}_D$. We first rewrite Eq.45 as

$$S_{LL}(t) = \frac{1}{2}\mathrm{Tr}\{R_t(t) I_L(0)\}. \tag{51}$$

The trace over the dot and the leads degrees of freedom can be performed by following the procedure used for the density matrix calculation. The resulting expression can be Fourier transformed via,

$$\tilde{S}_{LL}(\omega = 0) = 2\int_{-\infty}^{\infty} dt S_{LL}(t), \tag{52}$$

and we arrive at the zero frequency current noise ($U \to \infty$),

$$\begin{aligned} \tilde{S}_{LL}(\omega = 0) &= 2\sum_{q,p}\left[2(\tilde{R}(0)_q^0 + P_q^0) n_L((q-p)\omega_0)\Gamma_{q,p}^L\right. \\ &\quad \left. -(\tilde{R}(0)_q^1 - P_q^1)\bar{n}_L((q-p)\omega_0)\Gamma_{p,q}^L\right], \end{aligned} \tag{53}$$

where $\tilde{\mathbf{R}}(0)$ is the Fourier transform of vector $\mathbf{R}_D(t)$ at $\omega = 0$ and $\mathbf{R}_D(t)$ is given by

$$R_q^n(t) = \langle n, q|R_D(t)|n, q\rangle. \tag{54}$$

Here $\tilde{\mathbf{R}}(0)$ can be obtained, at steady state, via Eq.49.

$$\tilde{\mathbf{R}}(0) = -\mathcal{M}^{-1}\mathbf{h}. \tag{55}$$

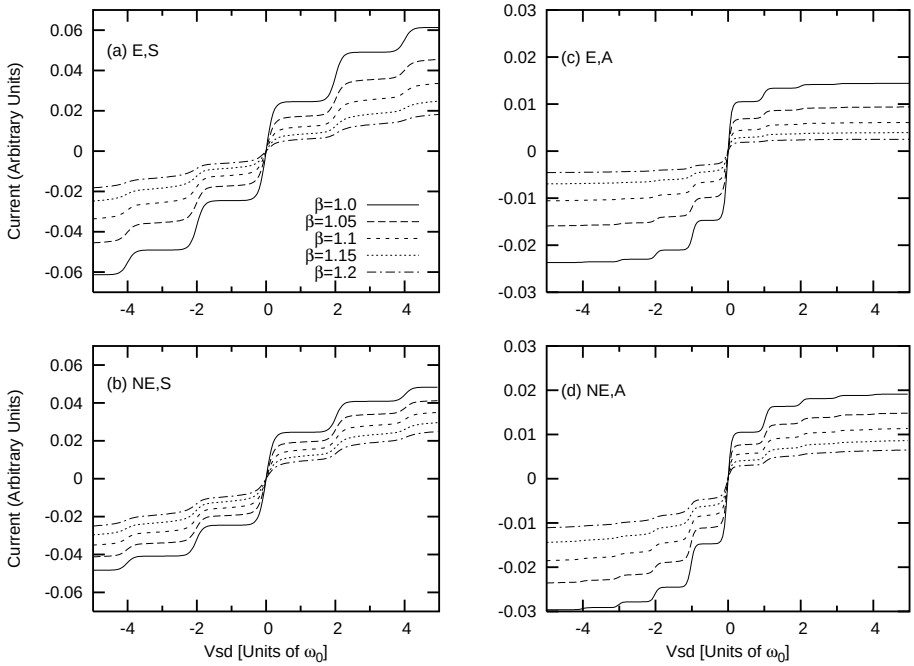

FIG. 1: Tunneling current plotted as a function of source-drain voltage with $\lambda = 1.0$. E and NE stand for equilibrated and non-equilibrated phonons respectively, and S and A stand for symmetric and asymmetric biases respectively. β is the exponent in the Luttinger-liquid distribution, which, in the noninteracting limit, is 1 and bigger than 1 for both repulsive and attractive interactions.

III. RESULTS

A. I-V characteristics

The tunneling current is obtained at steady state for both equilibrated and non-equilibrated phonons. Initially, the dot occupational probability vector, P_q^n, is numerically obtained via the rate equation (Eq.39). For equilibrated phonons, the ansatz, Eq.40, is used. The current is then numerically computed using Eq.43.

The current is plotted for three different electron-phonon coupling constants $\lambda = 0.5, 1.0, 2.0$. For each λ, current is computed under symmetric bias ($\mu_L = -\mu_R = V_{sd}/2$) and completely asymmetric bias ($\mu_R = 0$, $\mu_L = V_{sd}$) conditions and both equilibrated and unequilibrated phonon distributions are considered. Each plot consists of five plot-lines with different line styles. Each line style corresponds to a particular value of the exponent, β, in the Luttinger-liquid distribution function. The correspondence is shown in Fig.1(a). All other similar plots follow the same convention. All current plots are produced at $T = 0.05\omega_0$.

We first compare currents for equilibrated and non-equilibrated phonons. Mitra *et al.*[13] pointed out a peculiar behaviour in the current; near $\lambda = 1.0$ and with symmetric bias, the current is larger for equilibrated phonons than for non-equilibrated phonons. This is an unusual result since one would expect that phonons would arrange themselves so as to maximize the current in the non-equilibrium case. They attribute this peculiarity to the choice of λ at which many of the higher-order diagonal matrix elements (corresponding to q-phonon-q-phonon processes), Γ^i_{qq}, are suppressed. Although their work involved non-interacting leads, one can see in Fig.1 that this behaviour is observed also in the case of interacting leads. The behaviour, however, is not observed when $\lambda = 2$, consistent with Mitra *et al.*'s claim that this anomalous behaviour is pertinent to λ values close to 1.

The most apparent consequence of introducing interaction in the leads is the suppression of the tunneling current; the current decreases as interaction strength is raised. The question is whether the suppression of the current is mainly due to changes in the phonon distribution induced by electron interaction in the leads or a more direct consequence of the Luttinger-liquid distribution function. Fig.4 plots the phonon probability distribution for $\lambda = 1.0$. Upon careful inspection, a slight narrowing in the phonon distribution is observed; probabilities of dot states with low phonon numbers are increased while the wing of the distribution, corresponding to the dot states with high phonon numbers, is suppressed. Although they are not shown, the same subtle change in the phonon distribution is observed for other values of the electron-phonon coupling. However, because these changes are very small, the suppression in the current is unlikely due to the changes in the phonon distribution. Thus the main effect comes from

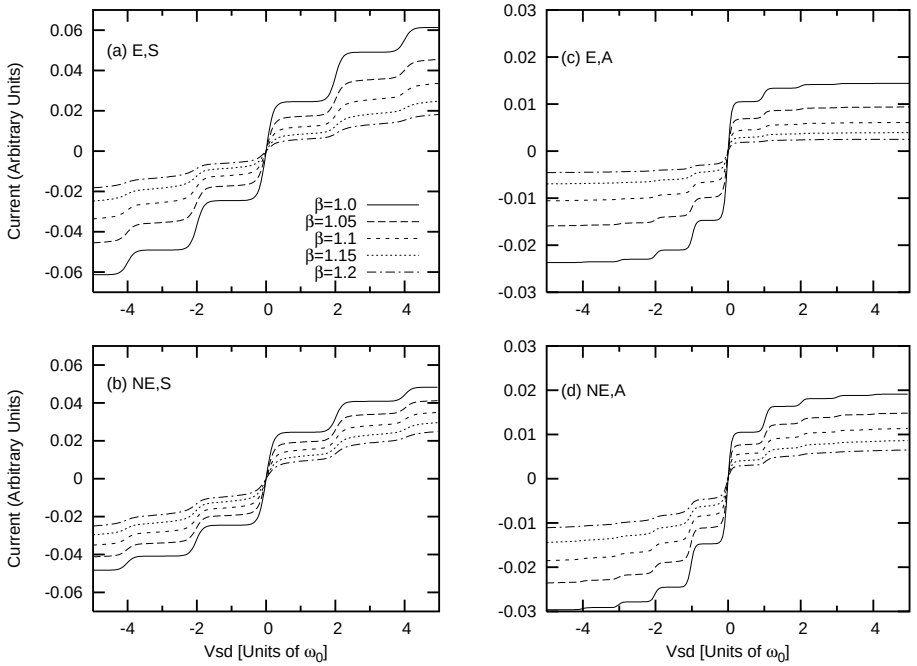

FIG. 2: Tunneling current plotted as a function of source-drain voltage with $\lambda = 0.5$.

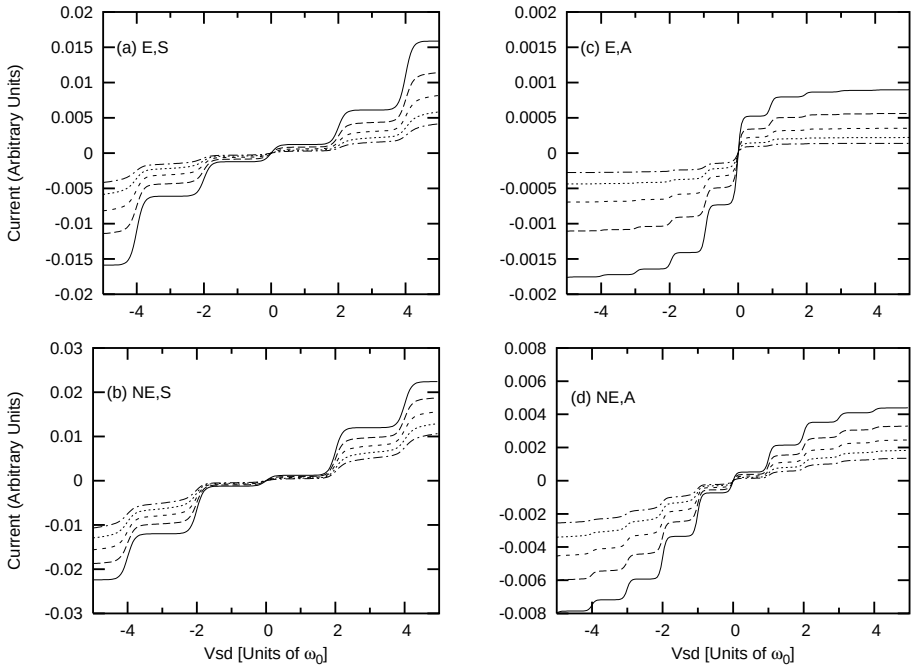

FIG. 3: Tunneling current plotted as a function of source-drain voltage with $\lambda = 2.0$.

the Luttinger-liquid distribution function that has replaced the Fermi distribution in the expression for the current (Eq.43). The Luttinger-liquid distribution function represents single-particle-like excitations decaying faster over time than non-interacting electrons. This results in the suppression of the overall current.

Although Fig.4 shows that the phonon distribution is not a strong function of electron interaction in the leads, Mitra *et al.*[13] showed that the phonon distribution is strongly affected by the electron-phonon coupling, λ. In particular, the distribution was farther from equilibrium for weak coupling than for strong coupling. We have observed that the phonon distribution strongly depends on the electron-phonon coupling even in the presence of intralead electron interaction. We conclude that varying the electron-phonon coupling has a much larger effect on the phonon distribution

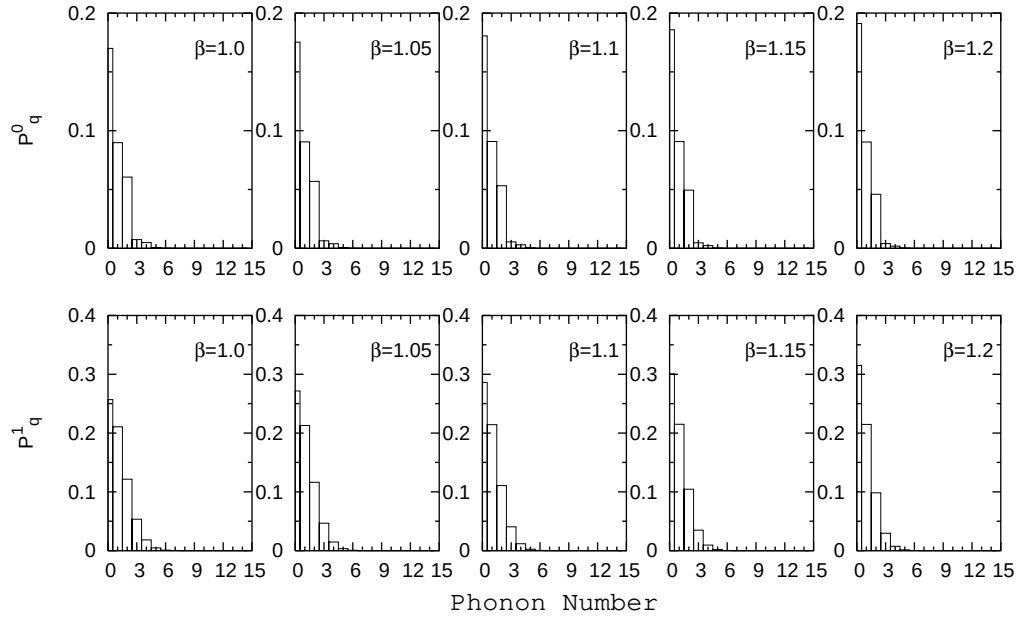

FIG. 4: Phonon probability distribution plotted with $\lambda = 1.0$ in the case of non-equilibrium phonons. Here, $\mu_L = -\mu_R = 2\omega_0$.

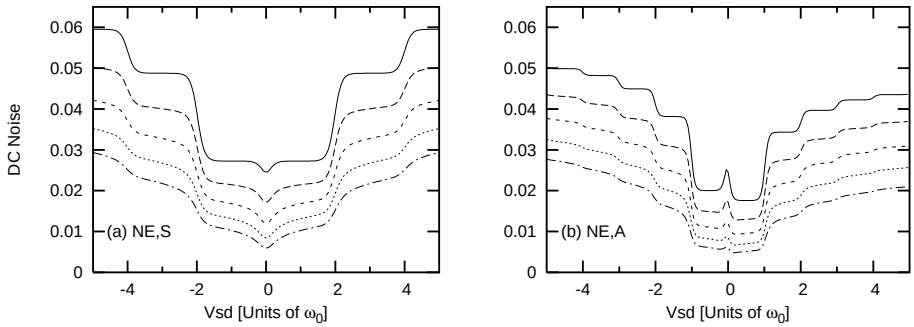

FIG. 5: DC noise plotted as a function of source-drain voltage with $\lambda = 1.0$.

than varying the interaction in the leads.

Another noticeable effect on the tunneling current due to interaction in the leads is the smearing and change in the slopes of the plateaus. These plateaus, which occur in a range of bias where the tunneling electrons encounter no new accessible excited state of the molecule, are flat in the case of non-interacting leads. However, as the interaction increases, the slopes also increase. This observation can be explained qualitatively in the zero-temperature limit, which is not the appropriate limit for this work but may give insight into this issue. The single-particle time correlation function for the Luttinger-liquid behaves as $1/t^{\beta}$. Fourier transform of this correlation function, which relates directly to $n(\omega)$, then behaves as $\omega^{\beta-1}$. Therefore, the current should show $V_{sd}^{\beta-1}$-type behaviour at low voltages. Each time you excite a new phonon, current should show $(V_{sd} - V_0)^{\beta-1}$-type behaviour, where V_0 is the voltage at which a new phonon is excited. Indeed, in the non-interacting limit, where $\beta = 1$, the slope is zero. However, when $\beta > 1$, the tilt and the smearing of the plateaus result.

B. DC noise characteristics

DC noise characteristics are obtained under both symmetric and asymmetric bias conditions for non-equilibrated phonons. The noise for equilibrated phonons is not presented here. In section III A, we argued that the modification in the current due to interaction in the leads is mainly due to the Luttinger-liquid nature of the electrons in the leads, not so much the induced change in the phonon distribution. For this reason, we anticipate that the effects of interaction on the DC noise for equilibrated phonons will be very similar for the case of non-equilibrated phonons.

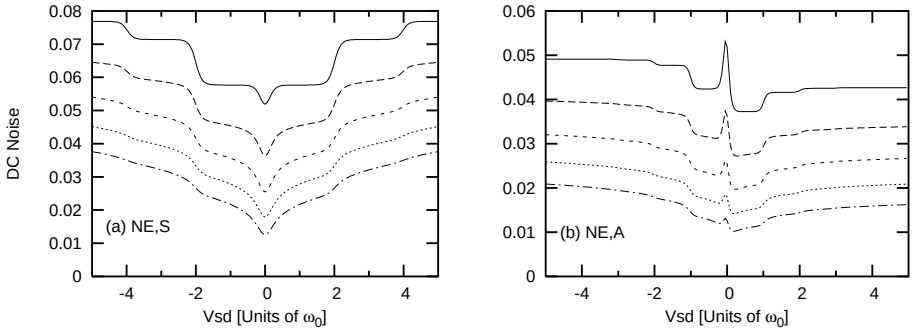

FIG. 6: DC noise plotted as a function of source-drain voltage with $\lambda = 0.5$.

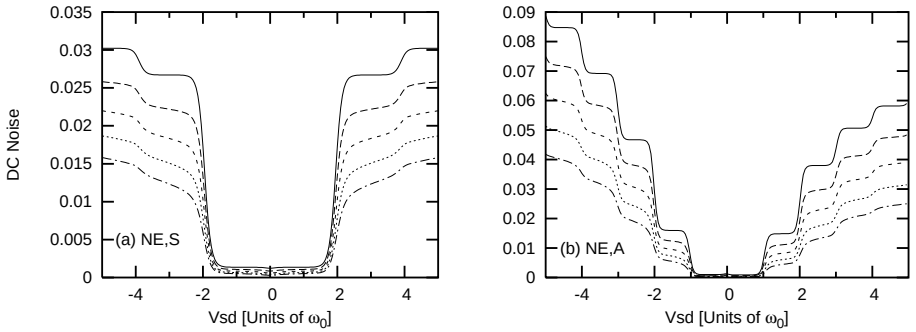

FIG. 7: DC noise plotted as a function of source-drain voltage with $\lambda = 2.0$.

The noise is plotted at the same three values of λ. The correspondence between the plot-line styles and the interaction parameters follow the same convention as in the plots for the current (see Fig.1). Figs.5-7 show that the noise is suppressed by interaction in the leads. This is expected since interaction in the leads causes tunneling events to be more correlated. The increase in correlation among subsequent tunneling events leads to decreased fluctuations and hence decreased current noise.

In Figs.8-10, we plot the current-normalized DC noise, or the Fano factor F,

$$F(V_{sd}) = \frac{S(V_{sd}) - S(V_{sd} = 0)}{2eI(V_{sd})}. \tag{56}$$

For all values of λ, electron interaction in the leads results in an increase in F. The plots also show that F depends dramatically on λ. In particular, F grows rapidly as λ increases[27], and is found to be super-Poissonian for $\lambda > 1$ (see Fig.10).

Fig.11 plots the noise at a higher temperature, $T = 0.1\omega_0$. Raising the temperature has a similar qualitative effect on the noise as increasing the interaction in the leads; the steps in the noise curve are smeared out and the plateaus between steps acquire a slope. However, the overall noise amplitude does not change when the temperature is raised while the amplitude decreases when the interaction is introduced.

IV. CONCLUSION

In this paper, we investigated the steady state current and the DC noise characteristics of a single level quantum dot coupled to two Luttinger liquid leads. In particular, we studied how the electron interaction in the leads and the coupling between tunneling electrons and on-dot phonons affect the dot's transport properties. We considered both equilibrium and out-of-equilibrium phonon distributions, and both symmetric and asymmetric bias orientations. The density matrix formalism was used to harness both phonon distributions in our calculations and to derive the semi-classical rate equation for the dot occupational probabilities. The calculations were done in the high-temperature approximation, in which the electron tunneling rate was assumed to be small enough so that the dot charge fluctuations are insignificant.

We have found that interaction in the leads in general suppresses the overall tunneling current and the noise, and smears out the steps in the I-V characteristics. This

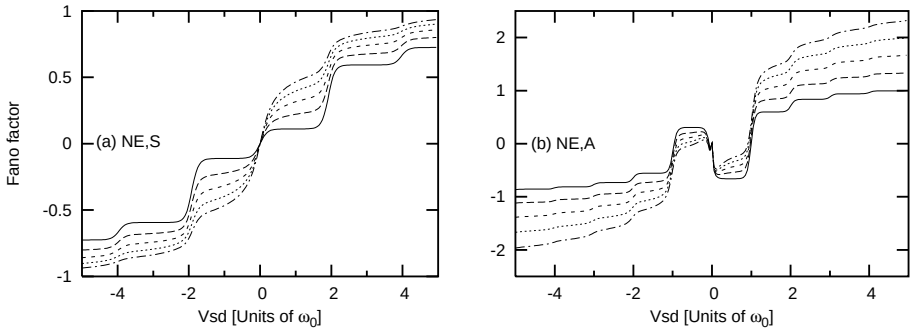

FIG. 8: Fano factor plotted as a function of source-drain voltage with $\lambda = 1.0$.

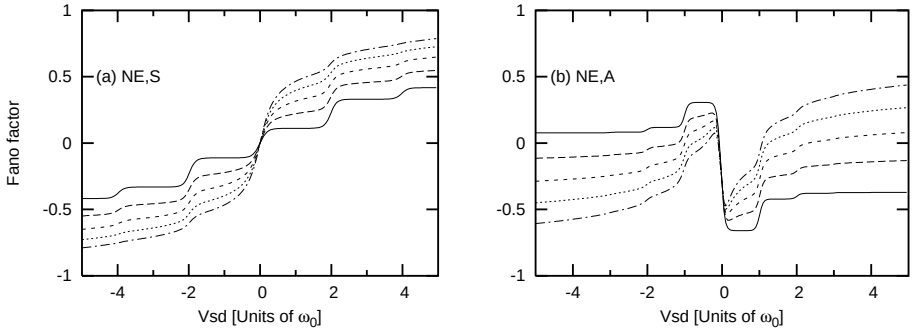

FIG. 9: Fano factor plotted as a function of source-drain voltage with $\lambda = 0.5$.

effect is mainly a consequence of the Luttinger-liquid correlation in the leads. The change in the phonon distribution of the dot due to electron-electron interaction in the leads is relatively small albeit we can see a slight narrowing of the phonon distribution as the interaction strength is increased, leading to only a minor contribution to the changes in current and noise. Comparing these behaviours of the current and noise with the effect of increased temperature, we find that increasing the temperature does not suppress overall current and noise even though it smears out the steps in I-V and noise characteristics. It is also found that the Fano factor, that represents the noise normalized by the current, becomes enhanced as the intralead electron interaction gets bigger. The Fano factor increases rapidly as the electron-phonon interaction becomes stronger and, interestingly, shows super-Poissonian behaviour as the electron-phonon coupling becomes greater than order one.

Acknowledgement: This work was supported by the NSERC of Canada, Canadian Institute for Advanced Research, Canada Research Chair Program, and OGS. We would like to thank Eugene Kim for earlier collaboration.

[1] R.H.M. Smit *et al.*, Nature **419**, 906 (2002).
[2] M.A. Reed, C. Zhou, C.J. Muller, T.P. Burgin, and J.M. Tour, Science **278**, 252 (1997).
[3] S. Datta, W. Tian, S. Hong, R. Reifenberger, J.I. Henderson, and C.P. Kubiak, Phys. Rev. Lett. **79**, 2530 (1997).
[4] D. Porath, Y. Levi, M. Tarabiah, and O. Millo, Phys. Rev. B **56**, 9829 (1997).
[5] L.A. Bumm *et al.*, Science **271**, 1705 (1996).
[6] J. Park, A.N. Pasupathy, J.I. Goldsmith, C. Chang, Y. Yaish, J.R. Petta, M. Rinkoski, J.P. Sethna, H. Abruna, P.L. McEuen, and D.C. Ralph, Nature (London) **17**, 722 (2002).
[7] M. Grobis, X. Lu, and M. F. Crommie, Phys. Rev. B **66**, 161408(R) (2002).
[8] C. Joachim, J.K. Gimzewski, and A. Aviram, Nature **408**, 541 (2000).
[9] A.N. Pasupathy, J. Clark, C. Chang, A.V. Soldatov S. Lebedkin, R.C. Bialczak, J.E. Grose, L.A.K. Donev, J.P. Sethna, D.C. Ralph, and P.L. McEuen, condmat/0311150.
[10] N.B. Zhitenev, H. Meng, and Z. Bao, Phys. Rev. Lett. **88**, 226801 (2002).
[11] B.C. Stipe, M.A. Razaei, and W. Ho, Science **280**, 1732 (1998).
[12] H. Park, J. Park, A.K.L. Lim, E.H. Anderson, A.P. Alivisatos, and P.L. McEuen, Nature (London) **407**, 57 (2000).
[13] A. Mitra, I. Aleiner, and A.J. Millis, Phys. Rev. B **69**, 245302 (2004).
[14] S. Braig and K. Flensberg, condmat/0401347 v1.
[15] K.D. McCarthy, N. Prokofiev, and M.T. Tuominen, Phys. Rev. B **67**, 245415 (2003).
[16] K. Flensberg, Phys. Rev. B **68**, 205323 (2003).

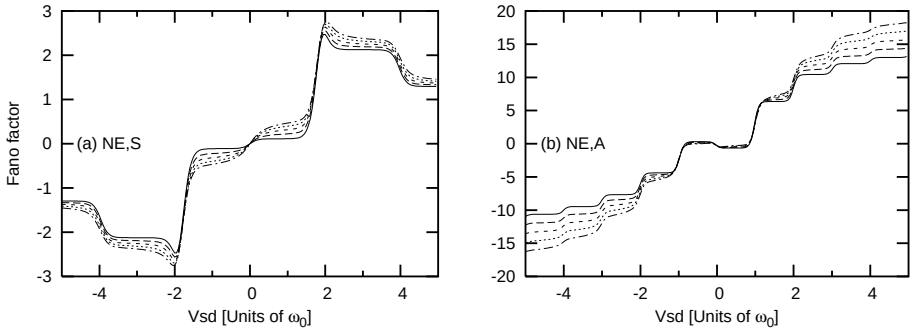

FIG. 10: Fano factor plotted as a function of source-drain voltage with $\lambda = 2.0$.

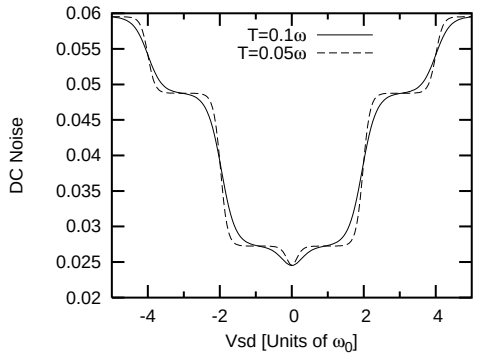

FIG. 11: DC noise plotted as a function of source-drain voltage with $\lambda = 1.0$ and $\beta = 1$ at two different temperatures.

[17] S. Braig and K. Flensberg, Phys. Rev. B **68**, 205324 (2003).
[18] V. Aji, J.E. Moore, and C.M. Varma, condmat/0302222 v2.
[19] U. Lundin and H. McKenzie, Phys. Rev. B **66**, 075303 (2002).
[20] D. Boese and H. Schoeller, Europhys. Lett. **54**, 668 (2001).
[21] N.S. Wingreen, K.W. Jacobsen, and J.W. Wilkins, Phys. Rev. B **40**, 011834 (1989).
[22] See section 4.3 in G.D. Mahan *Many-Particle Physics*, 2nd Edition (Plenum, New York, 1990).
[23] C.L. Kane, M.P.A. Fisher, Phys. Rev. Lett. **68**, 1220 (1992); Phys. Rev. B **46**, 15233 (1992).
[24] J. von Delft and H. Schoeller, condmat/9805275.
[25] H.J. Schulz, cond-mat/9503150.
[26] M.S. Dresselhaus, G. Dresselhaus, and P.C. Eklund *Science of Fullerenes and Carbon Nanotubes* (Academic, New York, 1996).
[27] Jens Koch and Felix von Oppen, cond-mat/0409667